Islanding-Aware Robust Energy Management for Microgrids

Yuanxiong Guo, *Member, IEEE*, and Chaoyue Zhao, *Member, IEEE*

***Abstract*—With the current trend of transforming a centralized power system into a decentralized one for efficiency, reliability, and environmental reasons, the concept of a microgrid that integrates a variety of distributed energy resources into distribution networks is gaining popularity. In this paper, we investigate the energy management of a microgrid with renewable energy sources (RESs), such as wind turbines and solar panels, and co-generation in both grid-connected and islanded modes. To address the uncertainties associated with RES power output and grid-connection condition in the microgrid, we propose a two-stage adaptive robust optimization approach to provide a robust unit commitment schedule for co-generation units, with the objective of minimizing the total operating cost under the worst-case scenario of renewable power output and grid-connection condition. The proposed approach ensures robust microgrid operation in consideration of worst-case scenarios, and the over-conservatism can also be mitigated by introducing "budget of uncertainty" parameters. Finally, a case study is conducted to show the effectiveness of the proposed approach.**

***Index Terms*—Microgrids, energy management, uncertainty, robustness, islanding.**

I. INTRODUCTION

DRIVEN by the benefits of increased energy efficiency brought by co-generation or combined heat and power (CHP), reduced carbon emissions, and improved power quality and reliability, distributed energy resources (DER) including distributed generation, distributed storage, and controllable loads are expected to play a significant role in future power systems. However, controlling a potentially large number of DER is very challenging for system operators to manage the power systems reliably and efficiently. By utilizing information and communication technologies in a localized distribution area, microgrids make it possible to coordinate DER and controllable loads efficiently to reduce the control burden on system operators [1]. A microgrid can operate in two modes: grid-connected mode and islanded mode. In grid-connected mode, the microgrid is connected to the main grid, and therefore is able to exchange power with the main grid to maintain its power balance. In case of disturbances in the main grid, the microgrid can be switched over to the islanded mode and operate autonomously. The islanding capability of the microgrid makes it an attractive option to address the reliability issue of traditional power grids and has received significant attention in both academia and industry.

Manuscript received October 2, 2015; revised January 8, 2016 and May 10, 2016; accepted June 22, 2016. Date of publication June 27, 2016; date of current version February 16, 2018. Paper no. TSG-01270-2015.

Y. Guo is with the School of Electrical and Computer Engineering, Oklahoma State University, Stillwater, OK 74078 USA (e-mail: richard.guo@okstate.edu).

C. Zhao is with the School of Industrial Engineering and Management, Oklahoma State University, Stillwater, OK 74078 USA (e-mail: chaoyue.zhao@okstate.edu).

Digital Object Identifier 10.1109/TSG.2016.2585092

Energy management is critical for reliable and efficient power systems operation and control. In traditional bulk power systems, the unit commitment and economic dispatch problems have been studied extensively to achieve the optimal energy management (see [2]–[4] for some recent results). However, compared with bulk power systems, the optimization of small-scale power systems, like microgrids, has important differences. One of the major differences is the presence of a local heat demand (e.g., district heating) in the microgrid, which adds another dimension to the optimization problem. Not only must the power demand be satisfied, but also the heat demand. Another difference is the impact of renewable energy sources (RES) units, such as solar panels and wind turbines, on the microgrid is much larger than that on bulk power systems due to the higher penetration level. Moreover, power demand in the microgrid usually contains some flexibility that can be leveraged for further optimization. Finally, the microgrid is able to switch between grid-connected mode and islanded mode in response to main grid disturbances, which should be considered in microgrid energy management.

Energy management in microgrids is receiving increasing attention due to its great importance in the future "Smart Grid". Specially, the economic dispatch problem for microgrids has been extensively studied. For instance, Zhang *et al.* [5] provide a robust approach to obtain the optimal economic dispatch in microgrids, but they do not either exploit the opportunity offered by adaptive recourse decisions or consider CHP systems for improving overall energy efficiency. Huang *et al.* [6] propose a real-time scheduling scheme based on the concept of quality-of-service in electricity, but only power demand is considered in this work. Zhou *et al.* [7] extend the model in [6] by considering both power and heat demand, but they disregard the unit commitment decisions which is important for microgrids. Lu *et al.* [8] propose several online algorithms for the microgrid generation scheduling problem with RES and co-generation. However, their method is limited to some special cases such as fast-responding generators. In addition, important factors such as storage and demand response can not be easily integrated into their framework. In contrast, our method is much more flexible and can incorporate many realistic operating constraints and components. Another related problem that has been studied extensively in literature is the energy management for co-generation systems (see [9] for a survey). However, the co-generation system is just one component of microgrids. Hence, we need to provide an integrated solution to energy management for microgrids. Robust optimization has been increasingly applied in several aspects of power system research to deal with uncertainty, such as security-constrained unit commitment [2], [4], [10], contingency-constrained unit commitment [11], PHEVs [12], and power grid interdiction [13]. However, none of them focus on the microgrid energy management. Recently, a resiliency-oriented microgrid optimal scheduling model is proposed in [14] using robust optimization. However, they formulate the normal operation and resilient operation of the microgrid separately. Also, CHP units are not considered and there is no discussion about the design of a proper uncertainty set to control the conservatism of the robust solution in their paper.

In this paper, we consider the energy management for a microgrid with RES, CHP, energy storage, and flexible demand in both grid-connected and islanded modes. Specifically, the microgrid energy management operates in two stages. First, the microgrid determines the day-ahead unit commitment schedule of its CHP units without knowing power output of RES and grid-connection condition. Then, after the RES power output and grid-connection condition are revealed, the microgrid dispatches its CHP and energy storage units, manages its controllable loads, and exchanges power with the main grid in real-time to meet both power and heat demand. To hedge against the uncertainties in RES power output and grid-connection condition, a robust optimization approach [15] is used. Using the robust optimization approach, the resulting unit commitment schedule is robust against all possible realizations of random RES power output and grid-connection condition in uncertainty sets. Our model ensures the microgrid to operate continually without load shedding when switching between the two modes. Moreover, to avoid over-conservatism of the robust optimization approach in handling uncertainties, we introduce "budget of uncertainty" parameters that provide trade-offs between robustness and optimality.

In summary, the main contributions of this paper are listed as follows.

1) We propose a novel two-stage robust optimization formulation to model the microgrid energy management problem considering CHP, RES, energy storage, flexible demand, and microgrid islanding. The proposed model can provide a robust unit commitment decision against any realizations of RES power output and grid-connection condition in uncertainty sets, and ensure the microgrid to switch between grid-connected mode and islanded mode seamlessly without load shedding.
2) By exploiting the special structure of the problem, we transform the two-stage robust optimization problem into a large-scale mixed integer linear program and develop an efficient decomposition approach to solve it iteratively in a tractable way.
3) We conduct a case study based on real datasets to verify the effectiveness of our proposed approach. Simulation results show the proposed approach is robust to uncertainties in RES power output and grid-connection condition, and offers a trade-off between robustness and optimality by choosing the proper "budget of uncertainty" parameters.

The rest of the paper is organized as follows. Section II describes the system model and assumptions used in the paper. Section III presents the mathematical formulation for the two-stage robust optimization problem. In Section IV, we propose an efficient solution method to solve the optimization problem. We conduct a case study in Section V and draw conclusions in Section VI.

II. System Modeling

Consider a microgrid which consists of CHP units, RES units, heat boilers, electricity storage (ES) units, thermal storage (TS) units, and power and heat loads. It is assumed that a central controller collects all the required information for energy management and performs centralized optimization in the microgrid. The energy management is over a finite time horizon $\mathcal{T} := \{1, 2, \ldots, T\}$ (e.g., 24 hours) with time period indexed by t.

A. Combined Heat and Power

CHP systems use the heat left over from generating power to produce either hot water which circulates through pipes to nearby buildings for heating, or steam which can be used for industrial purposes. The overall energy efficiency can be improved from 30% in power-only generation to 80% in CHP [16]. Denote the power output of CHP unit i at period t as $p_{i,t}$, which is restricted by its generating capacity:

$$\underline{P}_i I_{i,t} \le p_{i,t} \le \overline{P}_i I_{i,t}, \forall i, t. \tag{1}$$

Here $\underline{P}_i$ and $\overline{P}_i$ are the minimum and maximum power output of CHP unit i once it is turned on, respectively. The binary variable $I_{i,t}$ denotes the on/off status of CHP unit i at time t, where $I_{i,t} = 0$ if the unit is off and $I_{i,t} = 1$ if the unit is on. Moreover, we have the following ramping rate constraints of CHP units:

$$p_{i,t} - p_{i,t-1} \le u_{i,t}\overline{P}_i + (1 - u_{i,t})R^{\text{up}}_{i,p}, \forall i, t \tag{2}$$
$$p_{i,t-1} - p_{i,t} \le v_{i,t}\overline{P}_i + (1 - v_{i,t})R^{\text{dn}}_{i,p}, \forall i, t. \tag{3}$$

Here binary variables $u_{i,t}$ and $v_{i,t}$ take on a value of 1 if CHP unit i is being started up and shut down at time t, respectively, and $R^{\text{up}}_{i,p}$ and $R^{\text{dn}}_{i,p}$ are ramping up and down limits, respectively. Next, we have minimum on and off time constraints of CHP units, which are represented as:

$$I_{i,\tau} \ge u_{i,t}, \forall t, \tau \in \left[t, \min\left(T, t + T^{\text{up}}_i - 1\right)\right] \tag{4}$$
$$I_{i,\tau} \le 1 - v_{i,t}, \forall t, \tau \in \left[t, \min\left(T, T^{\text{dn}}_i - 1\right)\right] \tag{5}$$

where T^{up}_i and T^{dn}_i are minimum up and minimum down time periods. Finally, binary variables $I_{i,t}$, $u_{i,t}$ and $v_{i,t}$ are related as follows:

$$u_{i,t} - v_{i,t} = I_{i,t} - I_{i,t-1}, u_{i,t} + v_{i,t} \le 1, \forall i, t. \tag{6}$$

We assume a linear function $c_i^p p_{i,t} + c_i^{\text{on}} I_{i,t}$ for the operating cost of CHP unit i at time t. Moreover, the start-up and shut-down costs of CHP unit i at time t are represented as $c_i^{\text{su}} u_{i,t}$ and $c_i^{\text{sd}} v_{i,t}$, where c_i^{su} and c_i^{sd} represent the start-up cost and shut-down cost coefficients, respectively.

B. Heat Boiler

In practice, heat boilers are often used in conjunction with CHP units to add flexibility so that CHP units can be shut down during low heat demand periods. Without loss of generality, we assume the microgrid contains a single heat boiler. Moreover, we assume that the heat boiler can be turned on and off in a very short time so that we do not need to consider commitment decisions for it. Denote the heat generation of the boiler at period t as h_t^b, which is restricted by the maximum generation capacity $\overline{H}_b$, i.e.,

$$0 \leq h_t^b \leq \overline{H}_b, \forall t. \tag{7}$$

The fuel cost of using the boiler at time t can be represented as $c^b h_t^b$, where the coefficient c^b denotes the cost of generating one unit of heat energy from the boiler and is assumed to be time-invariant.

C. Energy Storage

In a microgrid with CHP and RES, both ES units and TS units are commonly used. Let $E_{m,t}^p$ denote the stored energy in ES unit m at the end of period t with initial available energy level $E_{m,0}^p$. Then, we have the following dynamics for the stored energy in ES unit m:

$$E_{m,t}^p = E_{m,t-1}^p + r_{m,t}^{p,+} \eta_m^{p,+} - r_{m,t}^{p,-} / \eta_m^{p,-}, \forall m, t, \tag{8}$$

where $r_{m,t}^{p,+}$ and $r_{m,t}^{p,-}$ are the charging and discharging rates of ES unit m at time t, respectively, and $\eta_m^{p,+}$ and $\eta_m^{p,-}$ represent the charging and discharging efficiencies of ES unit m, respectively. Since each ES unit has a finite capacity, then the stored energy in it has the following lower and upper bounds:

$$\underline{E}_m \leq E_{m,t}^p \leq \overline{E}_m, \forall m, t, \tag{9}$$

where the upper bound $\overline{E}_m$ is the storage capacity for ES unit m and the lower bound $\underline{E}_m$ is imposed to avoid the impact of deep discharging on the storage lifetime (e.g., 22% of the capacity for Li-ion batteries). Furthermore, ES units have charging and discharging rate limits as follows:

$$0 \leq r_{m,t}^{p,+} \leq R_m^{p,+}, 0 \leq r_{m,t}^{p,-} \leq R_m^{p,-}, \forall m, t, \tag{10}$$

where $R_m^{p,+}$ and $R_m^{p,-}$ denote the maximum charging and discharging rates for ES unit m, respectively. Lastly, without loss of generality, we assume that for each ES unit m, the final stored energy level should be the same as the initial stored energy level, i.e.,

$$E_{m,T}^p = E_{m,0}^p, \forall m. \tag{11}$$

Similarly, we have the following dynamics and operating constraints for TS units:

$$E_{n,t}^q = E_{n,t-1}^q + r_{n,t}^{q,+} \eta_n^{q,+} - r_{n,t}^{q,-} / \eta_n^{q,-}, \forall n, t \tag{12}$$

$$0 \leq r_{n,t}^{q,+} \leq R_n^{q,+}, 0 \leq r_{n,t}^{q,-} \leq R_n^{q,-}, \forall n, t \tag{13}$$

$$\underline{E}_n \leq E_{n,t}^q \leq \overline{E}_n, E_{n,T}^q = E_{n,0}^q, \forall n, t, \tag{14}$$

where $E_{n,t}^q$ denotes the stored energy at the end of the period t, $r_{n,t}^{q,+}(r_{n,t}^{q,-})$ denotes the charging (discharging) rate at period t, and $\eta_n^{q,+}(\eta_n^{q,-})$ denotes the charging (discharging) efficiency of TS unit n. Also, $R_n^{q,+}$ and $R_n^{q,-}$ are the maximum charging and discharging rates of TS unit n, respectively. Moreover, $\underline{E}_n$ and $\overline{E}_n$ are the minimum and maximum energy level of TS unit n, respectively. Finally, $E_{n,0}^q$ is the initial stored energy of TS unit n.

Since frequent charging and discharging would affect storage lifetime, we use $c_m^{\text{es}}(r_{m,t}^{p,+}\eta_m^{p,+} + r_{m,t}^{p,-}/\eta_m^{p,-})$ and $c_n^{\text{ts}}(r_{n,t}^{q,+}\eta_n^{q,+} + r_{n,t}^{q,-}/\eta_n^{q,-})$ to approximate the storage degradation costs, where c_m^{es} and c_n^{ts} represent the degradation cost coefficients of using ES unit m and TS unit n due to charging/discharging, respectively [17], [26].

D. Power and Heat Loads

The microgrid contains both power and heat loads, where power loads are further classified into two categories: static power loads and deferrable power loads. For static power loads, they are usually critical and there is no scheduling flexibility associated with their power profiles. We denote the aggregate power demand of all static loads as P_t^0 that must be satisfied at each period t.

For deferrable power loads, they only require a certain amount of electric energy to be delivered over a specified time interval and therefore, have some flexibility in their power profiles. Typical examples include electric vehicle (EV) charging and electric water heating. We model their total electric energy demand as L_j, where L_j for each deferrable load j has to be met within the time interval $[T_j^a, T_j^d]$. For each deferrable load j, the load serving rate $l_{j,t}$ must be in the required operation limits $[\underline{l}_j, \bar{l}_j]$. The deferrable load requirement is expressed as:

$$\sum_{t=T_j^a}^{T_j^d} l_{j,t} = L_j, \underline{l}_j \leq l_{j,t} \leq \bar{l}_j, \forall j, t \in \left[T_j^a, T_j^d\right] \tag{15}$$

$$l_{j,t} = 0, \forall j, t \notin \left[T_j^a, T_j^d\right]. \tag{16}$$

Since heat demand is usually inflexible, we assume that the aggregate heat demand Q_t is static and must be satisfied at each period t without interruption.

E. Grid-Connection Condition

As with [5], we assume that for the microgrid in grid-connected mode, the surplus power can be sold to the main grid with known selling price c_t^-, and the shortage power can be purchased from the main grid with known purchase price c_t^+ at each time period t. We further denote g_t^- and g_t^+ as the amount of power sold into and bought from the main grid at time t, respectively. Then, the market exchange cost of the microgrid with the main grid at time t can be represented as $c_t^+ g_t^+ - c_t^- g_t^-$.

Denote binary variables z_t as the grid-connection status at time t, and $\overline{g}$ as the power exchange line capacity between the microgrid and the main grid. We have

$$0 \leq g_t^- \leq \overline{g} z_t, 0 \leq g_t^+ \leq \overline{g} z_t, \forall t. \quad (17)$$

Note that when z_t is 0, the microgrid operates in islanded mode and cannot exchange power with the main grid. On the other hand, when z_t is 1, the microgrid operates in grid-connected mode and can purchase or sell power from or to the main grid up to the line capacity $\overline{g}$. However, the time and duration of islanding events are uncertain, and therefore z_t is random for all t.

F. Energy Balances

Since CHP units can generate useful heat and power simultaneously, we use a power-to-heat ratio α_i to represent the relationship between power and useful heat output of CHP unit i. That is, when one unit of power is generated, CHP unit i generates α_i unit of useful heat for free. Also, both power and heat must be balanced in all time periods for the microgrid. We use N_c, N_{es}, N_{ts} and N_j to denote the sets of CHP units, ES units, TS units, and deferrable loads, respectively. Then we have the following power balance equations:

$$\sum_{i=1}^{N_c} p_{i,t} + \sum_{m=1}^{N_{es}} \left(r_{m,t}^{p,-} - r_{m,t}^{p,+} \right) + w_t = g_t^- - g_t^+ + P_t^0 + \sum_{j=1}^{N_j} l_{j,t}, \forall t \quad (18)$$

where w_t denotes the aggregated RES power output in the microgrid and is uncertain.

For the heat balance equation, we have:

$$\sum_{i=1}^{N_c} \alpha_i p_{i,t}^s + \sum_{n=1}^{N_{ts}} \left(r_{n,t}^{q,-} - r_{n,t}^{q,+} \right) + q_t^b \geq Q_t, \forall t, \quad (19)$$

where we assume that all heat demand must be satisfied locally due to the fact that heat cannot be transported over a long distance, and surplus heat can be disposed without penalty.

G. Microgrid Operating Cost

Given the notations and assumptions above, the operating cost of the microgrid at each time period t can be represented as:

$$\begin{aligned} &\sum_{i=1}^{N_c} \left(c_i^{\text{su}} u_{i,t} + c_i^{\text{sd}} v_{i,t} + c_i^{\text{on}} I_{i,t} + c_i^p p_{i,t} \right) \\ &+ \sum_{m=1}^{N_{\text{es}}} c_m^{\text{es}} \left(r_{m,t}^{p,+} \eta_m^{p,+} + r_{m,t}^{p,-} / \eta_m^{p,-} \right) \\ &+ \sum_{n=1}^{N_{\text{ts}}} c_n^{\text{ts}} \left(r_{n,t}^{q,+} \eta_n^{q,+} + r_{n,t}^{q,-} / \eta_n^{q,-} \right) \\ &- c_t^- g_t^- + c_t^+ g_t^+ + c^b h_t^b. \end{aligned} \quad (20)$$

Note that in (20), the first line represents the operating cost of CHP units, the second and the third lines denote the degradation costs of ES and TS units, respectively, and the last line denotes the sum of the power exchange cost and the fuel cost of heat boiler.

III. Two-Stage Adaptive Robust Formulation

In this section, we first introduce two uncertainty sets to describe the RES power output uncertainty and grid-connection condition uncertainty, respectively. Then based on these uncertainty sets, we develop a two-stage adaptive robust formulation to model the islanding-aware microgrid energy management problem.

A. Uncertainty Set for RES Power Output

Note that the power balance equations (18) need to hold under the random RES power output w_t. To describe the RES power output uncertainty, instead of unrealistically assuming a particular probability distribution of the uncertain RES power output as required by the stochastic optimization approach, we only assume that the uncertain RES power output lies in a deterministic interval. We denote $\bar{w}_t$ as the forecasted value (i.e., nominal value) of the aggregate RES power output in period t. Then, its actual value of power output w_t in period t is assumed to be within an interval given by $[\bar{w}_t - \hat{w}_t^-, \bar{w}_t + \hat{w}_t^+]$, where $\hat{w}_t^-$ and $\hat{w}_t^+$ represent the maximum negative and positive deviations in period t, respectively. In practice, this interval can be estimated based on the confidence interval of RES power output such as 0.05 and 0.95 percentiles in [18].

However, robust optimization approach is usually too conservative. To overcome the conservativeness, we introduce an integer parameter Γ_w ($0 \leq \Gamma_w \leq T$) that restricts the number of periods that RES power output can deviate most from their nominal values (e.g., reaching either lower or upper bounds) across the scheduling horizon. This parameter is called the "budget of uncertainty" [19] in the robust optimization literature. Then, for simplicity of notations and without loss of generality, we assume the following cardinality constrained uncertainty set for the RES power output:

$$\mathcal{W} := \left\{ \mathbf{w} : w_t = \bar{w}_t + \hat{w}_t^+ \epsilon_t^+ - \hat{w}_t^- \epsilon_t^-, \forall t, \boldsymbol{\epsilon} \in \Lambda \right\}, \quad (21)$$

where

$$\Lambda := \left\{ \boldsymbol{\epsilon} : \sum_{t=1}^{T} \left(\epsilon_t^- + \epsilon_t^+ \right) \leq \Gamma_w, 0 \leq \epsilon_t^+, \epsilon_t^- \leq 1, \forall t \right\}. \quad (22)$$

The choice of Γ_w can adjust the conservativeness of the robust solution. Specifically, if Γ_w is 0, then there is no uncertainty in RES power output, while if Γ_w is T, the RES power output can reach its lower/upper limit in every period over the scheduling horizon, corresponding to the most conservative case.

B. Uncertainty Set for Grid-Connection Condition

The microgrid can be switched over to islanded mode when a disturbance occurs in the main grid and be resynchronized back with the main grid when the disturbance is resolved. Without appropriate planning, the microgrid might have to curtail some local loads to maintain energy balance when switching from grid-connected mode to islanded mode. Therefore, the central controller has to ensure that all local power and heat demand can be satisfied without interruption under all possible disturbance scenarios.

As mentioned before, in order to capture the uncertainty associated with the main grid disturbances, we use a binary variable z_t to represent the grid-connection condition. To overcome the conservativeness, we define another "budget of uncertainty" parameter $0 \leq \Gamma_g \leq T$ to restrict the number of periods that the microgrid can be islanded from the main grid. Then, the uncertainty set for the grid-connection condition can be shown as follows:

$$\mathcal{Z} := \left\{ \mathbf{z} : \sum_{t=1}^{T} (1 - z_t) \leq \Gamma_g, z_t \in \{0, 1\}, \forall t \right\}. \tag{23}$$

The choice of Γ_g controls the conservativeness of the robust solution. Specifically, if Γ_g is 0, the microgrid is assumed to be operated only in grid-connected mode, while if Γ_g is T, the microgrid is assumed to be operated only in islanded mode for the whole scheduling horizon. More detailed modeling of the grid-connection condition is possible by adding additional constraints into (23).

C. Robust Optimization Formulation

With uncertainty sets for RES power output and grid-connection condition defined above, we develop a two-stage adaptive robust optimization formulation to determine the robust day-ahead CHP unit commitment decisions for the microgrid. In the first stage, we make the unit commitment decisions of CHP units when the RES power output and grid-connection condition are uncertain. Then in the second stage, after the worst-case scenario of RES power output and grid-connection condition is realized, we make the dispatch-related decisions of energy resources in the microgrid to minimize the dispatch cost. The decisions of the two stages are related through the generating power level and ramping rate constraints of CHP units (1)–(3). The model is called adaptive because the second-stage decisions are made after uncertainties are revealed and therefore adaptive to any realization of the uncertainties. Thus, this two-stage adaptive robust optimization problem is formulated as follows:

$$\begin{aligned}\min_{\mathbf{u},\mathbf{v},\mathbf{I}} \Bigg\{ & \sum_{t=1}^{T} \sum_{i=1}^{N_c} \left(c_i^{\mathrm{su}} u_{i,t} + c_i^{\mathrm{sd}} v_{i,t} + c_i^{\mathrm{on}} I_{i,t} \right) \\ & + \max_{\mathbf{w} \in \mathcal{W}, \mathbf{z} \in \mathcal{Z}} \min_{\mathbf{p},\mathbf{h},\mathbf{r},\mathbf{g},\mathbf{l}} \sum_{t=1}^{T} \Bigg[\sum_{i=1}^{N_c} c_i^p p_{i,t} + c_t^+ g_t^+ - c_t^- g_t^- \\ & + c_{\mathrm{b}} h_t^{\mathrm{b}} + \sum_{m=1}^{N_{\mathrm{es}}} c_m^{\mathrm{es}} \left(r_{m,t}^{p,+} \eta_m^{p,+} + r_{m,t}^{p,-} / \eta_m^{p,-} \right) \\ & + \sum_{n=1}^{N_{\mathrm{ts}}} c_n^{\mathrm{ts}} \left(r_{n,t}^{q,+} \eta_n^{q,+} + r_{n,t}^{q,-} / \eta_n^{q,-} \right) \Bigg] \Bigg\}, \end{aligned} \tag{24}$$

subject to constraints (1)–(19).

IV. Solution Methodology

In the following, we develop a method to solve the above adaptive robust optimization problem efficiently. For simplicity of presentation, we write the two-stage robust optimization problem in a matrix form:

$$\min \quad \mathbf{c}^T \mathbf{x} + \max_{\mathbf{w} \in \mathcal{W}, \mathbf{z} \in \mathcal{Z}} \min_{\mathbf{y} \in \Omega(\mathbf{x},\mathbf{w},\mathbf{z})} \mathbf{d}^T \mathbf{y}(\mathbf{x}, \mathbf{w}, \mathbf{z}) \tag{25}$$

$$\text{s.t.} \quad \mathbf{A}\mathbf{x} \leq \mathbf{b}, \mathbf{x} \in \{0, 1\} \tag{26}$$

$$\Omega(\mathbf{x}, \mathbf{w}, \mathbf{z}) = \Big\{ \mathbf{F}\mathbf{y} \leq \mathbf{g}, \tag{27}$$

$$\mathbf{Q}\mathbf{y} \leq \mathbf{r} - \mathbf{P}\mathbf{x}, \tag{28}$$

$$\mathbf{T}\mathbf{y} = \mathbf{w}, \tag{29}$$

$$\mathbf{R}\mathbf{y} \leq \mathbf{z} \Big\}, \tag{30}$$

where $\Omega(\mathbf{x}, \mathbf{w}, \mathbf{z})$ is the set of feasible dispatch decisions for a fixed commitment decision $\mathbf{x}$ as well as RES power output realization $\mathbf{w}$ and grid-connection condition indicator $\mathbf{z}$. In the matrix form, the vector $\mathbf{x}$ represents the first-stage decisions and the vector $\mathbf{y}$ represents the second-stage decisions. The objective function (25) is split into two parts: one depends on the commitment decisions and the other depends on the dispatch decisions. Equation (26) collects all constraints involving only commitment variables (4)–(6). Equation (27) accounts for constraints (7)–(16) and (19). Constraints (1)–(3) that involve both commitment decisions and dispatch decisions are grouped in (28). Equation (29) represents the constraints (18) that involve uncertain RES power output. Equation (30) contains the information of constraints (17), which is related to the uncertain grid-connection condition.

A. Problem Reformulation

To solve the above two-stage robust optimization problem, we first find the dual of the innermost minimization problem by observing that it is a linear program and strong duality holds, and transform the second-stage problem into the following:

$$\begin{aligned} \max_{\mathbf{w},\mathbf{z},\boldsymbol{\lambda},\boldsymbol{\mu},\boldsymbol{\varphi},\boldsymbol{\sigma}} \quad & -\boldsymbol{\lambda}^T \mathbf{g} - \boldsymbol{\mu}^T (\mathbf{r} - \mathbf{P}\mathbf{x}) + \boldsymbol{\varphi}^T \mathbf{w} - \boldsymbol{\sigma}^T \mathbf{z} \\ \text{s.t.} \quad & -\boldsymbol{\lambda}^T \mathbf{F} - \boldsymbol{\mu}^T \mathbf{Q} + \boldsymbol{\varphi}^T \mathbf{T} - \boldsymbol{\sigma}^T \mathbf{R} = \mathbf{d}^T \\ & \boldsymbol{\lambda} \geq 0, \boldsymbol{\mu} \geq 0, \boldsymbol{\sigma} \geq 0, \mathbf{w} \in \mathcal{W}, \mathbf{z} \in \mathcal{Z}, \end{aligned} \tag{31}$$

where $\boldsymbol{\lambda}$, $\boldsymbol{\mu}$, $\boldsymbol{\varphi}$, and $\boldsymbol{\sigma}$ are the Lagrangian multipliers of the constraints (27), (28), (29), and (30), respectively. Then we further transform it into a linear form using the Big-M method [10]. First, due to the bilinear structure of the objective function and the fact that uncertainty set $\mathcal{W}$ is independent of all other variables in the above formulation, the optimal solution $\mathbf{w}^*$ must be extreme points of $\mathcal{W}$. Therefore, for all t,

$$w_t^* = \bar{w}_t + \hat{w}_t \epsilon_t^+ - \hat{w}_t \epsilon_t^-, \sum_{t=1}^{T} \left(\epsilon_t^+ + \epsilon_t^- \right) \leq \Gamma_w \tag{32}$$

where ϵ_t^+ and ϵ_t^- are binary variables. Substituting (32) into the bilinear term $\boldsymbol{\varphi}^T \mathbf{w}$, we have

$$\boldsymbol{\varphi}^T \mathbf{w} = \sum_{t=1}^{T} \left(\varphi_t \bar{w}_t + \varphi_t \epsilon_t^+ \hat{w}_t - \varphi_t \epsilon_t^- \hat{w}_t \right). \tag{33}$$

Next, by defining auxiliary variables π_t^+, π_t^-, ξ_t^+ and ξ_t^-, we can transform the second-stage problem into the following:

$$\begin{aligned}
\max_{\boldsymbol{\lambda},\boldsymbol{\mu},\boldsymbol{\varphi},\boldsymbol{\sigma},\boldsymbol{\epsilon},\boldsymbol{\pi},\boldsymbol{\xi},\mathbf{z}} \quad & -\boldsymbol{\lambda}^T\mathbf{g} - \boldsymbol{\mu}^T(\mathbf{r} - \mathbf{P}\mathbf{x}) + \sum_{t=1}^{T}(\varphi_t\bar{w}_t \\
& + \pi_t^+\hat{w}_t^+ + \pi_t^-\hat{w}_t^-) + \sum_{t=1}^{T}(\xi_t^+ + \xi_t^-)\overline{g}_t \\
\text{s.t.} \quad & -\boldsymbol{\lambda}^T\mathbf{F} - \boldsymbol{\mu}^T\mathbf{Q} + \boldsymbol{\varphi}^T\mathbf{T} - \boldsymbol{\sigma}^T\mathbf{R} = \mathbf{d}^T \\
& \boldsymbol{\lambda} \geq 0, \boldsymbol{\mu} \geq 0, \boldsymbol{\sigma} \geq 0 \\
& \pi_t^+ \leq M\epsilon_t^+, \pi_t^+ \leq \varphi_t + M(1-\epsilon_t^+), \forall t \\
& \pi_t^- \leq M\epsilon_t^-, \pi_t^- \leq -\varphi_t + M(1-\epsilon_t^-), \forall t \\
& \xi_t^+ \leq Mz_t, \xi_t^+ \leq -\sigma_t^+ + M(1-z_t), \forall t \\
& \xi_t^- \leq Mz_t, \xi_t^- \leq -\sigma_t^- + M(1-z_t), \forall t \\
& \sum_{t=1}^{T}(\epsilon_t^+ + \epsilon_t^-) \leq \Gamma_w, \sum_{t=1}^{T}(1-z_t) \leq \Gamma_g \\
& \epsilon_t^+, \epsilon_t^-, z_t \in \{0,1\}, \forall t, \qquad (34)
\end{aligned}$$

where M is a sufficiently large constant. Note that the above formulation is a mixed-integer linear program (MILP) which can be readily solved by commercial solvers.

B. Column-and-Constraint Generation Algorithm

We have shown that the worst-case scenarios of RES power output can only occur at the extreme points of its uncertainty set, and therefore are finite. Hence, we denote $\{(\mathbf{w}_k, \mathbf{z}_k), k = 1, 2, \ldots, K\}$ as the extreme points of the joint set $\mathcal{W} \times \mathcal{Z}$. Moreover, we assign a copy of the recourse decision variables $\mathbf{y}_k$ to each of these extreme points. In principle, we can enumerate all these possible worst-case scenarios and write the equivalent form of the two-stage robust optimization problem as the following large-scale mixed-integer linear program:

$$\begin{aligned}
\min_{\mathbf{x},\theta,\mathbf{y}_k|_{k\leq K}} \quad & \mathbf{c}^T\mathbf{x} + \theta && (35a) \\
\text{s.t.} \quad & \mathbf{A}\mathbf{x} \leq \mathbf{b}, \mathbf{x} \in \{0,1\} && (35b) \\
& \theta \geq \mathbf{d}^T\mathbf{y}_k, k = 1, 2, \ldots, K && (35c) \\
& \mathbf{F}\mathbf{y}_k \leq \mathbf{g}, k = 1, 2, \ldots, K && (35d) \\
& \mathbf{Q}\mathbf{y}_k \leq \mathbf{r} - \mathbf{P}\mathbf{x}, k = 1, 2, \ldots, K && (35e) \\
& \mathbf{T}\mathbf{y}_k = \mathbf{w}_k, k = 1, 2, \ldots, K && (35f) \\
& \mathbf{R}\mathbf{y}_k \leq \mathbf{z}_k, k = 1, 2, \ldots, K. && (35g)
\end{aligned}$$

However, in practice it is difficult for even the state-of-the-art optimization solvers to locate the optimal solution in a tractable time. Therefore, we employ a variant of Benders decomposition, called Column-and-Constraint Generation (C&CG) algorithm [20] to solve it. It has been shown in [20] that the C&CG algorithm is guaranteed to converge to the optimal solution in a finite number of iterations when solving the above form of two-stage robust optimization problems and is significantly superior to the traditional Benders decomposition method [21] in terms of convergence speed.

The C&CG algorithm is described below:

Step 1: Let $\mathbf{x}_0$ be a feasible first-stage decision. Solve the sub problem (34) with $\mathbf{x}$ fixed at $\mathbf{x}_0$. Let $\mathbf{w}_1$ and $\mathbf{z}_1$ be the worst-case scenario of RES power output and grid-connection condition in the optimal solution. Set the upper bound UB $= +\infty$, the lower bound LB $= -\infty$, and the iteration index $i \leftarrow 1$.

Step 2: Define the master problem as the minimization of the objective function (35a) subject to constraints (35b)–(35g), and solve the master problem. Let $(\mathbf{x}_i, \theta_i)$ be the optimal solution. Update LB $= \mathbf{c}^T\mathbf{x}_i + \theta_i$.

Step 3: Solve the sub problem (34) with $\mathbf{x}$ fixed at $\mathbf{x}_i$. Let $\mathbf{w}_{i+1}$ and $\mathbf{z}_{i+1}$ be the worst-case scenario of RES power output and grid-connection condition in the optimal solution and ρ^* be the optimal objective function value. Update UB $= \min\{\text{UB}, \mathbf{c}^T\mathbf{x}_i + \rho^*\}$.

Step 4: If UB$-$LB $< \varepsilon$, where ε is a small tolerance value, then stop. Otherwise, update $i \leftarrow i+1$ and go back to Step 2.

V. Case Study

In this section, we present the results of a case study by evaluating the proposed algorithm with real datasets. We apply the proposed robust approach to a microgrid and compare the performances of stochastic and robust optimization approaches. All the experiments are implemented in Python [22] using GUROBI 6.0 [23] on a desktop with an Intel Core i7-4770 3.4 GHz CPU and 8GB of memory. The convergence tolerance value ε for the decomposition algorithm is set to 10^{-2}.

A. Microgrid Description

The considered microgrid includes three CHP units, a wind farm, a heat boiler, an EV battery bank, a hot water tank, a heat load, a base power load, and a deferrable power load. The parameters of the three CHP units are collected from [24] with the heat to power ratio set to 1.2. Also, the day-ahead forecasted value of wind power output $\bar{w}_t$ is taken from [25] where coefficients are appropriately scaled. We assume a symmetric interval, i.e., $\hat{w}_t^+ = \hat{w}_t^-$, and set them to $0.8\bar{w}_t$ for each period t. Additionally, we have a heat boiler system with the maximum heat output of 5000kWh. The unit heat generation cost c^{h} is set to 0.0205$/kWh. Moreover, we have an EV battery bank consisting of six identical Li-ion EV batteries deployed in the microgrid. Each EV battery has a storage capacity of 30kWh, and both its charging and discharging efficiencies are 0.9. The maximum charge and discharge rates are set to 16kW. To prolong the battery lifetime, the energy level should never drop below 22% of its capacity. Both the initial and final stored electrical energy levels are set to 50% of the total capacity. The battery degradation cost coefficient c_m^{es} is set to 0.0035$/kWh [26]. Similarly, the hot water tank has a total capacity of 250kWh with charging and discharging efficiencies of 0.9 and it can be operated with the maximum charging and discharging rates of 100kW. Both the initial and final stored heat energy levels are set to 50% of the total capacity. The hot water tank degradation cost coefficient c_n^{ts} is set

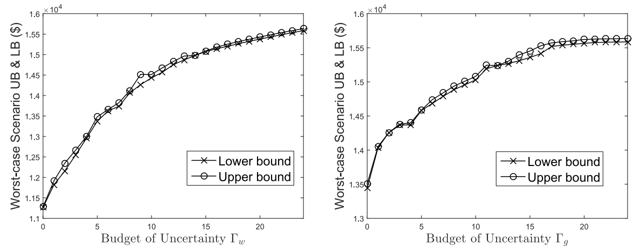

(a) (b)

Fig. 1. The lower and upper bounds of the C&CG algorithm with different "budget of uncertainty" parameters Γ_w and Γ_g.

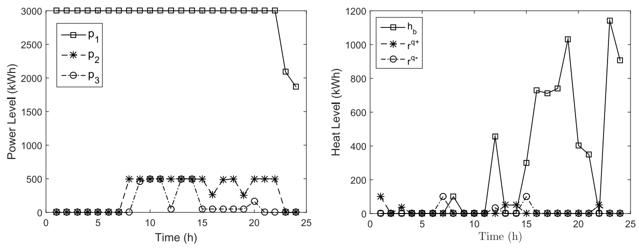

(a) (b)

Fig. 2. (a) Power generation levels for CHP units. (b) Heat boiler output and TS charging and discharging decisions.

to 0.0035$/kWh. In addition, we use the historic dataset as the forecasted total power demand [27] where coefficients are appropriately scaled. The deferrable load has a total demand of 300kWh. The maximum and minimum load serving rates are 150kW and 10kW, respectively. The start time and end time of the deferrable load are set to 10th and 20th periods, respectively. The electricity prices are taken from [28] with coefficients appropriately scaled. Finally, the selling price c_t^- is set to 80% of the purchasing price c_t^+. The power exchange line capacity is set to 4000kW. We introduce a linear penalty cost function for the unsatisfied power demand that results in load shedding, and the unit penalty cost is set to 10$/kWh.

B. Results and Discussion

1) Convergence of C&CG Algorithm: We first test the convergence property of the proposed C&CG algorithm under different budgets of uncertainty $\Gamma_w, \Gamma_g \in [0, 24]$. Fig. 1(a) and Fig. 1(b) show the lower and upper bounds obtained by the proposed algorithm as Γ_w and Γ_g range from 0 to 24, respectively. The iteration number needed for convergence under all cases is two to six showing that the proposed algorithm converges fast.

2) Solutions of Our Approach: The robust optimal UC decisions and the worst-case scenario of wind power output and grid connection under $\Gamma_g = 2$ and $\Gamma_w = 6$ are collected in Table I. As we can see from the table, in the worst-case scenario, the wind power output reaches its lower bound from 9h to 11h and from 20h to 22h, and the grid is disconnected in 23h and 24h. The corresponding second-stage decisions under the worst-case scenario are shown in Fig. 2 and Fig. 3.

3) Efficiency, Reliability, and Robustness of Our Approach: We test the solutions of the proposed robust approach for three sets of randomly generated scenarios to check the efficiency and reliability of our approach, and find out the proper budgets of uncertainty to avoid over-conservatism. The performance of our adaptive robust approach are evaluated in three aspects: 1) the average operating cost, 2) the volatility (i.e., standard deviation) of the operating cost, and 3) the sensitivity of the operating cost to different probability distributions of the uncertain wind power output and grid-connection condition. The average operating cost refers to the optimality of the first-stage decision; the volatility of the operating cost indicates the reliability of the second-stage decision under the first-stage decision; and the third aspect shows the robustness of the first-stage decision against the wind power output and grid-connection condition probability distributions.

First, we evaluate the impact of uncertain wind power output on the operating cost. The microgrid is assumed to operate in islanded mode for the whole operating day. Two sets of 1000 randomly sampled wind power output scenarios are generated, one following a uniform distribution in the interval $[\bar{w}_t - \hat{w}_t^-, \bar{w}_t + \hat{w}_t^+]$ and the other following

TABLE I
ROBUST OPTIMAL SOLUTION OF THE MICROGRID

Period	$I_{1,t}$	$I_{2,t}$	$I_{3,t}$	w_t(kW)	z_t
1	1	0	0	757.7320	1
2	1	0	0	649.4845	1
3	1	0	0	644.3299	1
4	1	0	0	577.3196	1
5	1	0	0	649.4845	1
6	1	0	0	572.3196	1
7	1	0	0	680.4124	1
8	1	1	0	618.5567	1
9	1	1	1	128.8660	1
10	1	1	1	115.4639	1
11	1	1	1	83.5052	1
12	1	1	1	355.6701	1
13	1	1	1	298.9691	1
14	1	1	1	329.8969	1
15	1	1	1	438.1443	1
16	1	1	1	520.6186	1
17	1	1	1	587.6289	1
18	1	1	1	742.2680	1
19	1	1	1	819.5876	1
20	1	1	1	170.1031	1
21	1	1	0	181.4433	1
22	1	1	0	174.2268	1
23	1	0	0	829.8969	0
24	1	0	0	706.1856	0

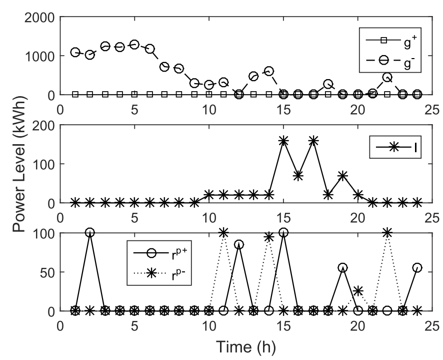

Fig. 3. Grid power exchange, deferrable load scheduling and ES charging and discharging decisions.

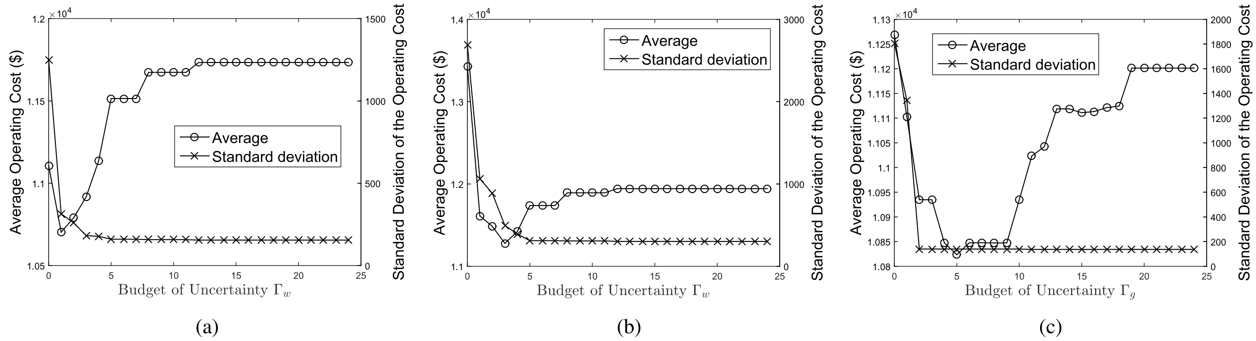

Fig. 4. The average and standard deviation of the microgrid operating cost for (a) normally distributed wind power output, (b) uniformly distributed wind power output, and (c) Bernoulli distributed grid-connection condition.

a normal distribution with mean $\bar{w}_t$ and standard deviations $(\hat{w}_t^+ + \hat{w}_t^-)/6$. Samples that fall outside of the feasible region $[0, w_{\max}]$ in the normal distribution case are truncated. Fig. 4(a) and Fig. 4(b) show the average and standard deviation of the operating cost for different budgets of uncertainty Γ_w under these two scenario sets. We observe that the average operating costs are the lowest for $\Gamma_w = 1$ and $\Gamma_w = 3$ under normally and uniformly distributed wind power output scenarios, respectively. We also observe that the standard deviation of the operating cost reduces significantly when Γ_w is small and becomes steady at last.

Second, we test the impact of uncertain grid-connection condition on the operating cost. This is to show the capability of our approach in handling different grid-connection conditions. The wind power output of the microgrid is set to the minimum level for the whole operating day in this simulation. Fig. 4(c) shows the average operating costs with 1000 grid-connection condition scenarios generated from Bernoulli distribution for different budgets of uncertainty Γ_g. We observe that when the budget of uncertainty Γ_g is 5, the microgrid has the lowest average operating cost. In addition, we also compare the standard deviation of each budget of uncertainty Γ_g. We observe that the standard deviation of the operating cost reduces fast until Γ_g increases to 2 and becomes steady thereafter. From the above simulation results, it can be observed that with proper choices of budgets of uncertainty, our robust approach can ensure the robustness and optimality of the solution at the same time.

4) Comparison With the Stochastic Programming Approach: In this part, we compare our robust approach with the stochastic programming approach in solving the microgrid energy management problem. Note that the stochastic programming approach has been widely used in handling uncertainty in previous works on microgrid energy management (see [26] and its cited references). For the robust approach, we set $\Gamma_w = 6$ and $\Gamma_g = 2$. For the stochastic programming approach, 400 scenarios are drawn from the truncated normal distribution with mean $\bar{w}_t$ and standard deviation $(\hat{w}_t^+ + \hat{w}_t^-)/6$ to model the wind power uncertainty and the Bernoulli distribution to model the grid-connection uncertainty. Scenarios exceeding the uncertainty budgets are discarded. Using these scenarios, the first-stage decisions are obtained for the stochastic programming approach. Next, a validation set of 1000 scenarios, which are drawn from the same distributions as the ones used in the stochastic programming approach, is used to calculate the dispatch cost of the robust and stochastic programming approaches. The results are summarized in Table II. As we can observe, the commitment cost is higher for the robust approach since it takes a conservative action to handle the uncertainties by turning on more units. In total, the stochastic approach outperforms the robust approach in terms of average cost by about 4.24%. However, the stochastic approach incurs a worst-case cost as high as 1.72 times the worst-case cost with the robust approach.

TABLE II
COMPARISON OF SYSTEM COST WITH THE ROBUST OPTIMIZATION AND THE STOCHASTIC PROGRAMMING APPROACHES

	Robust Approach	Stochastic Approach
Commitment Cost ($)	2496	1579
Average Dispatch Cost ($)	6856.1	7376.4
Worst-Case Dispatch Cost ($)	7963.9	16432
Average Total Cost ($)	9352.1	8955.4
Worst-Case Total Cost ($)	10460	18011

VI. CONCLUSION

An efficient model for islanding-aware robust energy management of a microgrid with renewable energy sources and co-generation in both grid-connected and islanded mode has been proposed. A two-stage adaptive robust optimization approach has been developed with the objective of providing a robust unit commitment schedule for co-generation units that minimizes the total operating cost under the worst-case renewable power output and grid-connection condition. The proposed optimization approach handles the uncertainties in both renewable power output and grid-connection condition. A Column-and-Constraint Generation algorithm has been employed to solve the robust optimization problem efficiently. The proposed approach has been analyzed through a case study with real datasets. Simulation results show that our approach is both reliable and efficient. Moreover, with properly chosen "budget of uncertainty" parameters, our robust approach can ensure robustness and optimality of the solution at the same time.

REFERENCES

[1] N. Hatziargyriou, H. Asano, R. Iravani, and C. Marnay, "Microgrids," *IEEE Power Energy Mag.*, vol. 5, no. 4, pp. 78–94, Jul./Aug. 2007.

[2] L. Zhao and B. Zeng, "Robust unit commitment problem with demand response and wind energy," in *Proc. IEEE Power Energy Soc. Gen. Meeting*, San Diego, CA, USA, 2012, pp. 1–8.

[3] Q. Wang, Y. Guan, and J. Wang, "A chance-constrained two-stage stochastic program for unit commitment with uncertain wind power output," *IEEE Trans. Power Syst.*, vol. 27, no. 1, pp. 206–215, Feb. 2012.

[4] D. Bertsimas, E. Litvinov, X. Sun, J. Zhao, and T. Zheng, "Adaptive robust optimization for the security constrained unit commitment problem," *IEEE Trans. Power Syst.*, vol. 28, no. 1, pp. 52–63, Feb. 2013.

[5] Y. Zhang, N. Gatsis, and G. B. Giannakis, "Robust energy management for microgrids with high-penetration renewables," *IEEE Trans. Sustain. Energy*, vol. 4, no. 4, pp. 944–953, Oct. 2013.

[6] Y. Huang, S. Mao, and R. M. Nelms, "Adaptive electricity scheduling in microgrids," in *Proc. INFOCOM*, Turin, Italy, 2013, pp. 1142–1150.

[7] K. Zhou, J. Pan, and L. Cai, "Optimal combined heat and power system scheduling in smart grid," in *Proc. INFOCOM*, Toronto, ON, Canada, 2014, pp. 2831–2839.

[8] L. Lu, J. Tu, C.-K. Chau, M. Chen, and X. Lin, "Online energy generation scheduling for microgrids with intermittent energy sources and co-generation," in *Proc. ACM SIGMETRICS*, 2013, pp. 53–66.

[9] F. Salgado and P. Pedrero, "Short-term operation planning on cogeneration systems: A survey," *Elect. Power Syst. Res.*, vol. 78, no. 5, pp. 835–848, 2008.

[10] R. Jiang, J. Wang, and Y. Guan, "Robust unit commitment with wind power and pumped storage hydro," *IEEE Trans. Power Syst.*, vol. 27, no. 2, pp. 800–810, May 2012.

[11] Q. Wang, J.-P. Watson, and Y. Guan, "Two-stage robust optimization for n-k contingency-constrained unit commitment," *IEEE Trans. Power Syst.*, vol. 28, no. 3, pp. 2366–2375, Aug. 2013.

[12] A. H. Hajimiragha, C. A. Canizares, M. W. Fowler, S. Moazeni, and A. Elkamel, "A robust optimization approach for planning the transition to plug-in hybrid electric vehicles," *IEEE Trans. Power Syst.*, vol. 26, no. 4, pp. 2264–2274, Nov. 2011.

[13] L. Zhao and B. Zeng, "Vulnerability analysis of power grids with line switching," *IEEE Trans. Power Syst.*, vol. 28, no. 3, pp. 2727–2736, Aug. 2013.

[14] A. Khodaei, "Resiliency-oriented microgrid optimal scheduling," *IEEE Trans. Smart Grid*, vol. 5, no. 4, pp. 1584–1591, Jul. 2014.

[15] D. Bertsimas, D. B. Brown, and C. Caramanis, "Theory and applications of robust optimization," *SIAM Rev.*, vol. 53, no. 3, pp. 464–501, 2011.

[16] *Efficiency Benefits*. Accessed on Aug. 15, 2015. [Online]. Available: http://www.epa.gov/ chp/basic/efficiency.html

[17] S. B. Peterson, J. F. Whitacre, and J. Apt, "The economics of using plug-in hybrid electric vehicle battery packs for grid storage," *J. Power Sources*, vol. 195, no. 8, pp. 2377–2384, 2010.

[18] D. Bertsimas, V. Gupta, and N. Kallus, "Data-driven robust optimization," Oper. Res. Center, Massachusetts Inst. Technol., Cambridge, MA, USA, Tech. Rep., 2013. [Online]. Available: https://arxiv.org/abs/1401.0212

[19] D. Bertsimas and M. Sim, "The price of robustness," *Oper. Res.*, vol. 52, no. 1, pp. 35–53, 2004.

[20] B. Zeng and L. Zhao, "Solving two-stage robust optimization problems using a column-and-constraint generation method," *Oper. Res. Lett.*, vol. 41, no. 5, pp. 457–461, 2013.

[21] J. F. Benders, "Partitioning procedures for solving mixed-variables programming problems," *Numer. Math.*, vol. 4, no. 1, pp. 238–252, 1962.

[22] *Python*. Accessed on Sep. 1, 2015. [Online]. Available: https://www.python.org/

[23] *GUROBI*. Accessed on Sep. 1, 2015. [Online]. Available: http://www.gurobi.com/

[24] S. X. Chen, H. B. Gooi, and M. Q. Wang, "Sizing of energy storage for microgrids," *IEEE Trans. Smart Grid*, vol. 3, no. 1, pp. 142–151, Mar. 2012.

[25] *National Wind Technology Center M2 Tower*. Accessed on Feb. 3, 2015. [Online]. Available: http://www.nrel.gov/midc/nwtc_m2/

[26] D. T. Nguyen and L. B. Le, "Optimal bidding strategy for microgrids considering renewable energy and building thermal dynamics," *IEEE Trans. Smart Grid*, vol. 5, no. 4, pp. 1608–1620, Jul. 2014.

[27] J. Wang, M. Shahidehpour, and Z. Li, "Security-constrained unit commitment with volatile wind power generation," *IEEE Trans. Power Syst.*, vol. 23, no. 3, pp. 1319–1327, Aug. 2008.

[28] *PJM—Markets and Operations*. Accessed on Feb. 3, 2015. [Online]. Available: http://www.pjm.com/markets-and-operations.aspx

Yuanxiong Guo (M'14) received the B.Eng. degree in electronics and information engineering from the Huazhong University of Science and Technology, Wuhan, China, in 2009, and the M.S. and Ph.D. degrees in electrical and computer engineering from the University of Florida, Gainesville, FL, USA, in 2012 and 2014, respectively. Since 2014, he has been an Assistant Professor with the School of Electrical and Computer Engineering, Oklahoma State University, Stillwater, OK, USA. His research interests include big data and cyber-physical energy systems. He received the Best Paper Award from the IEEE Global Communications Conference in 2011.

Chaoyue Zhao (M'12) received the B.S. degree in information and computing sciences from Fudan University, China, in 2010, and the Ph.D. degree in industrial and systems engineering from the University of Florida, in 2014. She is an Assistant Professor of Industrial Engineering and Management with Oklahoma State University, Stillwater, OK, USA. Her research interests include data-driven stochastic optimization and stochastic integer program with their applications on power grid security and renewable energy management.